Eur Radiol (2006) 16: 2161–2178
DOI 10.1007/s00330-006-0161-1

R. Schmitt
S. Froehner
G. Coblenz
G. Christopoulos

Carpal instability

Received: 8 August 2005
Revised: 29 December 2005
Accepted: 13 January 2006
Published online: 1 March 2006

R. Schmitt (✉) · S. Froehner · G. Coblenz · G. Christopoulos
Herz- und Gefäßklinik GmbH,
Institut für Diagnostische und Interventionelle Radiologie,
Salzburger Leite 1, 97616
Bad Neustadt an der Saale, Germany
e-mail: schmitt.radiologie@herzchirurgie.de
Tel.: +49-9771-662901
Fax: +49-9771-659215

Abstract This review addresses the pathoanatomical basics as well as the clinical and radiological presentation of instability patterns of the wrist. Carpal instability mostly follows an injury; however, other diseases, like CPPD arthropathy, can be associated. Instability occurs either if the carpus is unable to sustain physiologic loads ("dyskinetics") or suffers from abnormal motion of its bones during movement ("dyskinematics"). In the classification of carpal instability, dissociative subcategories (located within proximal carpal row) are differentiated from non-dissociative subcategories (present between the carpal rows) and combined patterns. It is essential to note that the unstable wrist initially does not cause relevant signs in standard radiograms, therefore being "occult" for the radiologic assessment. This paper emphasizes the high utility of kinematographic studies, contrast-enhanced magnetic resonance imaging (MRI) and MR arthrography for detecting these predynamic and dynamic instability stages. Later in the natural history of carpal instability, static malalignment of the wrist and osteoarthritis will develop, both being associated with significant morbidity and disability. To prevent individual and socio-economic implications, the handsurgeon or orthopedist, as well as the radiologist, is challenged for early and precise diagnosis.

Keywords Dysfunction · Wrist · Magnetic resonance imaging · Kinematography · Instability

Introduction

The wrist is an exceedingly complex and versatile structure. Built out of several small carpal joints, it allows a substantial degree of motion in the coronal and sagittal planes, and enables with the radioulnar joints three-dimensional rotatory movements around the longitudinal axis of the forearm [1]. Its construction, as well as the wide range of motion, makes the wrist susceptible to axial forces and deforming vectors. Nevertheless, the intact wrist remains remarkably stable [2] and is able to sustain external stress forces. The considerable stability of the wrist is mainly attained by the principle of the "dynamic support" [3].

Carpal stability may be described as the ability of the wrist to maintain a normal balance between the articulating partners under physiologic loads and movements. In "equilibrium", any external force is answered by a counterforce to restore the original joint status without yielding or losing joint congruency [4–6]. However, if the counterforces are insufficient to keep the normal articular arrangement, the balance of the articulating partners may be disturbed.

The term "carpal instability"—in 1972 introduced by Linscheid et al. [7]—has undergone modifications in the past. Nowadays, the most accepted definition of "carpal instability" means any disturbance of the static and dynamic balance of forces at the wrist under the conditions

of daily living [8]. The degree of carpal instability is determined by the extent of the ligamentary and/or osseous lesions. “Dynamic” instability describes a deformity only occuring during motion, whereas “static” instability is already seen with the wrist at rest.

The objective of this review is to illustrate the pathological, clinical and radiological aspects of carpal instability.

Osseous anatomy

Distal forearm

The carpal bones are interposed between the forearm and the metacarpus. The antebrachial glenoid is formed by the articular surfaces of the radius and the triangular fibrocartilage complex (TFCC). The radial articular surface, which carries the triangular scaphoid fossa and the rectangular lunate fossa, is tilted ulnarly in about 23 degrees (range 15–35 degrees) and volarly in about 11 degrees (range 0–20 degrees) [9].

Proximal carpal row

The bones of the proximal carpal row (scaphoid, lunate and triquetrum) represent the carpal condyle, which is in close articular congruence with the antebrachial glenoid. There are some special features. Firstly, the scaphoid is double-obliquely aligned at angles of about 45 degrees with respect to both the coronal and sagittal planes (Fig. 1). Both, its oblique orientation and its length, which exceeds the midcarpal axis make the scaphoid comparable with slider crank [7, 10]. Secondly, in comparison to the lunate, the proximal articular surface of the scaphoid is more curved, allowing the scaphoid to rotate more extensively [11]. Thirdly, the subunits of the proximal row move with significant degrees of rotation in relation to each other. Fourthly, the configuration of the lunate is coronally wedge-shaped, explaining its inherent tendency toward displacing into extension when dissociated from the scaphoid [12].

Distal carpal row

The bones of the distal carpal row (trapezium, trapezoid, capitate and hamate) form together a solitary functional unit with only minimal intercarpal movement. Both carpal rows are connected via the midcarpal joint. This joint is composed of three different joints: the convex-concave scaphotrapezoid-trapezial (STT) and scaphocapitate compartments laterally, as well as the capitatolunate compartment centrally, and the semihelicoidal hamatotriquetral compartment medially [12, 13]. The midcarpal articulation approximates a ball-and-socket joint with the inherent tendency of the capitate to intrude into the scapholunate gap.

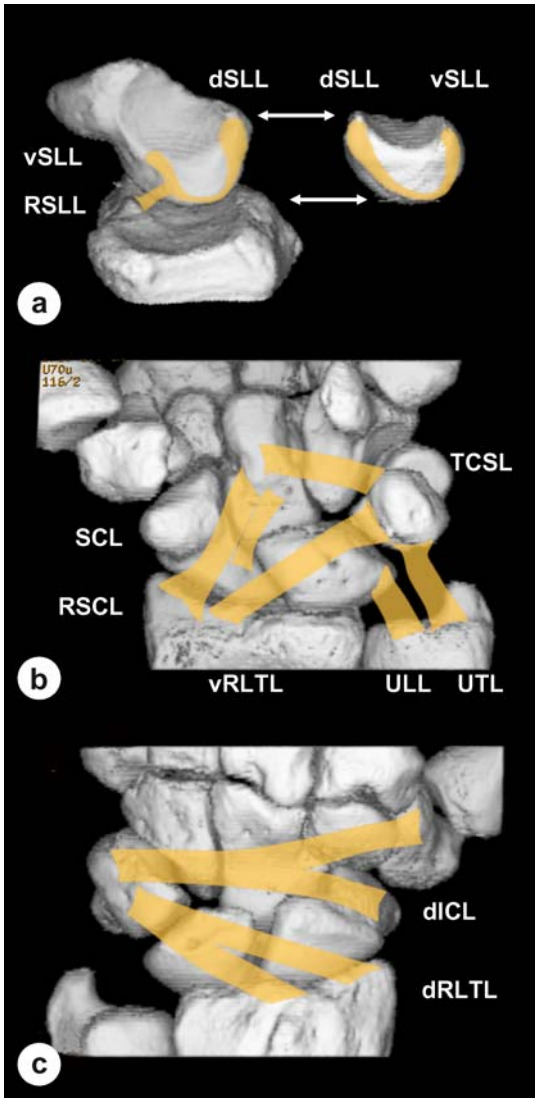

Fig. 1a–c Schematic illustration of the carpal ligaments. The ligaments are depicted in *yellow* on 3D images of a CT data set reconstructed with the surface shaded display (SSD) mode. **a** Anatomy of the U-shaped SLL. The scaphoid is seen from medially after the other carpals have been removed (*left*), whereas the lunate is mirror-inverted and seen from laterally (*right*). *RSLL* radioscapholunate ligament, *vSLL* volar segment of the scapholunate ligament, *dSLL* dorsal segment of the scapholunate ligament. **b** Anatomy of the volar carpal ligaments. The ligaments are oriented like two inverted “V” analogues. Proximal volar “V-ligaments”: *vRLTL* volar radiolunotriquetral ligament, *ULL* ulnolunate ligament, *UTL* ulnotriquetral ligament. Distal volar “V-ligaments”: *RSCL* radioscaphocapitate ligament, *SCL* scaphocapitate ligament, *TCSL* triquetrocapitatoscaphoid (“arcuate”) ligament (the lateral part is omitted for a better overview). **c** Anatomy of the dorsal carpal ligaments. The ligaments are oriented like “V” analogues rotated around 90 degrees (*dRLTL* dorsal radiolunotriquetral ligament, *dICL* dorsal intercarpal ligament)

Ligamentous anatomy

The anatomy of the carpal ligaments follows the principles of Table 1 [6, 14]. (1) Ligaments are usually subdivided into intraarticular stabilizers (the interosseous SLL and LTL, and the midcarpal ligaments) and intracapsular stabilizers (ligaments integrated in the capsular sheaths), respectively. (2) The intracapsular ligaments run either intrinsic (both, the origin and insertion within the carpus) or extrinsic (connecting the forearm with the carpus). (3) From the functional point of view, it is reasonable to differentiate interosseous ligaments (travelling deeply in transverse courses) and the so-called "V-ligament" system (ligaments travelling superficially in oblique courses).

Intrinsic interosseous ligaments

Scapholunate interosseous ligament

The scapholunate interosseous ligament (SLL) is most important. It bends like a horseshoe in sagittal extension between the peripheral borders of the scaphoid and lunate (Fig. 1a). Both the dedicated construction and the elasticity of the SLL permit a moderate rotational movement between the scaphoid and lunate during flexion and extension according to their different articular curvatures. The SLL has three segments with different biomechanic functions [15, 16]. (1) The volar SLL segment extends in an oblique-transverse direction in the coronal plane. This portion is longer than the other two allowing the scaphoid and lunate to move slightly at the volar level [4]. It consists of collagen fibers embedded in loose connective tissue. (2) The middle SLL segment, which extends in the transaxial plane, is a fibrocartilaginous membrane without any stabilizing function. The central portion is predisposed to degenerative perforations. (3) The dorsal SLL segment is comprised of closely-packed collagenous fibers running horizontally in the coronal plane. The thick and relatively short dorsal portion ensures the stability of the scapholunate compartment [4, 15, 17]. Therefore, the rupture of the dorsal SLL segment is imperative for the development of symptomatic scapholunate dissociation (SLD) and the rotatary subluxation of the scaphoid (RSS). The so-called "secondary stabilizers" of the scapholunate compartment must be mentioned. These supporting structures initially prevent a dissociation even when SLL is completely ruptured. Important secondary stabilizers are the volar STTL, the RSCL, the SCL and the flexor carpi radialis (FCR) tendon [2, 17].

Lunotriquetral interosseous ligament

The lunotriquetral interosseous ligament (LTL) is constructed similar to the SLL; however, it is of smaller size [18]. The LTL is also U-shaped. (1) The strong volar LTL segment ensures the functional stability within the lunotriquetral compartment. This portion consists of thick collagenous fascicles that extend horizontally in the coronal plane. (2) The middle LTL segment is a thin, transaxial membrane without any stabilizing function. This portion is preferred for degenerative perforations. (3) The dorsal LTL segment, which is composed of thin horizontal fascicles, contributes less to articular stability. The lunotriquetral compartment is supported by secondary stabilizers, mainly the extrinsic volar and dorsal radiolunotriquetral ligaments (vRLTL, dRLTL).

Table 1 Synoptic anatomy of the most important ligaments of the wrist. The ligaments are listed with respect of their positions and courses within the wrist. Additionally, the main function is listed in the right column (*PCR* proximal carpal row)

Position	Ligament	Abbrev.	Function
Interosseous	Scapholunate ligament	SLL	PCR stabilizer
	Lunotriquetral ligament	LTL	PCR stabilizer
	Radioscaphoid ligament	RSL	Volar scaphoid stabilizer
	Radioscapholunate ligament (Testut)	RSLL	Neurovascular bundle
	Radiolunate ligament (short RL ligament)	RLL	Volar lunate stabilizer
Volar proximal V	Volar radiolunotriquetral ligament (long RL ligament)	vRLTL	Radiocarpal stabilizer ("slingshot")
	Ulnotriquetral ligament	UTL	Ulnocarpal stabilizer
	Ulnolunate ligament	ULL	Ulnocarpal stabilizer
Volar distal V	Radioscaphocapitate ligament	RSCL	Radiocarpal and scaphoid stabilizer ("slingshot", "supporter")
	Scaphocapitate ligament	SCL	Midcarpal stabilizer
	Triquetrocapitatoscaphoid (arcuate) lig.	TCSL	Midcarpal stabilizer
	Scaphotrapeziotrapezoidal ligament	STTL	Scapholunate stabilizer
Dorsal V	Dorsal radiolunotriquetral ligament	dRLTL	Radiocarpal stabilizer ("slingshot")
	Dorsal intercarpal ligament	dICL	Midcarpal stabilizer

Extrinsic interosseous ligaments

There are three short ligaments on the volar side of the wrist interposed between the intrinsic interosseous ligaments and the volar V-shaped ligaments. Both the radioscaphoid ligament (RSL) and the radiolunate ligament (RLL, "short radiolunate") reinforce the volar joint capsule. The RSL prevents the scaphoid from dorsal subluxation [19], while the RLL tautly stabilizes the lunate. The radioscapholunate ligament (RSLL, Testut's) is believed to be a neurovascular bundle carrying terminal branches of the anterior interosseous artery and the anterior interosseous nerve to supply the SLL and the proximal scaphoid pole [20].

Extrinsic V-ligaments

Volar V-ligament complexes

The volar V-shaped complex is built of thick intracapsular ligaments [14, 20]. Two groups can be differentiated: the proximal V-ligaments and the distal V-ligaments [6], both separated by Poirier's space, an area free of ligaments on the volar aspect of the lunocapitate articulation (Fig. 1b).

On the lateral leg of the "proximal V", the volar radiolunotriquetral ligament (vRLTL, "long radiolunate") originates on the distal radius, runs first to the lunate, and terminates on the triquetrum [21]. Due to its oblique course the vRTDL is part of the so-called "articular slingshot". The medial leg of the "proximal V" consists of the ulnolunate ligament (ULL) and the ulnotriquetral ligament (UTL), both fortifying the medial carpus and the TFCC. They originate on the volar side of the TFCC and proceed to the lunate and triquetrum, respectively.

The lateral leg of the "distal V" is composed of three elements [21]. The radioscaphocapitate ligament (RSCL) originates at the radial styloid process and extends diagonally, first through a volar groove in the scaphoid and then inserts on the capitate. The RSCL, which is separated from the scaphoid waist by a synovial duplication, provides a fulcrum for the rotation of the scaphoid and keeps it in a stable, volar-flexed position (so-called "volar support band") [6]. It is accompanied by the scaphocapitate ligament (SCL), which stabilizes the midcarpal joint, too. Finally, the scaphotrapeziotrapezoid ligament (STTL) serves as the "radial link" of the wrist by connecting the three lateral carpals. The medial leg of the "distal V" is formed by the triquetrocapitatoscaphoid ligament (TCSL). This "arcuate" ligament originates on the triquetrum, extends fan-shaped over the proximal hamate and capitate, and terminates on the distal scaphoid [22]. The TCSL crosses and stabilizes the midcarpal joint together with the SCL and the STTL. Its triquetrocapitate portion, the so-called "ulnar link", is a fairly loose structure that permits the triquetrum to slide over the helicoid hamatotriquetral joint [2]. On the contrary, the capitatoscaphoid portion is tight.

Dorsal V-ligament complex

The dorsal V-shaped complex is weaker than the volar ligament complex (Fig. 1c). There are no dorsal ligaments between the ulna and the carpal bones [14, 21]. The extrinsic dorsal radiolunotriquetral ligament (dRLTL) extends from Lister's tubercle of the radius diagonally to the triquetrum, thereby crossing the proximal scaphoid pole and the lunate [6]. The intrinsic dorsal intercarpal ligament (dICL) takes a horizontal course. It originates at the triquetrum, crosses the capitate and the STT joints, and terminates on the scaphoid, trapezium and trapezoid bones [6]. All dorsal ligaments converge at the triquetrum, thus not only stabilizing the radiocarpal joint, but also the lunate and the capitate from dorsal [16].

The stabilizers of the wrist

Stable arrangement of the carpal bones at rest and under load is based on the geometry of their articular surfaces, the tension of the linking ligaments and the actual contraction state of the muscles involved.

Stabilizers of the radiocarpal joint

Stability of the radiocarpal joint is ensured volarly by the RSCL and vRLTL, and dorsally by the dRLTL (Fig. 1b,c). The oblique orientation of these "slingshot" ligaments, which course from proximal-radial origins to distal-ulnar insertions, prevents the carpus to slide down along the ulnar and volar tilts of the radius [23]. Such "translocation" instability is mainly caused by an injury of the radiocarpal ligaments and by rheumatoid arthritis [6, 23, 24].

Stabilizers of the proximal carpal row

The proximal carpal row is stabilized by the SLL and the LTL (Fig. 1a). The intrinsic ligaments do not simply connect the proximal carpals in a straight course. Intraligamentary torsion forces are additionally caused by opposing rotational torques between the scaphoid, lunate

and triquetrum leading to further coaptation of the proximal carpal row. Injuries of these ligaments cause scapholunate and lunotriquetral dissociation (SLD and LTD), respectively (so-called "dissociative" instability) [7, 18].

Stabilizers of the midcarpal joint

The midcarpal joint is stabilized by transversely crossing ligaments, volarly by the ulnar branch of the TCSL and the SCL (Fig. 1b), and dorsally by the dICL (Fig. 1c) [2]. These ligaments do not simply connect both carpal rows, but they also ensure the proximal row to smoothly move from flexion to extension as the wrist deviates ulnarly. If these midcarpal stabilizers get insufficient, then any axial load pushes the proximal row into flexion, mainly because of the obliquely oriented midcarpal joint surfaces (so-called "midcarpal" instability) [7].

Stabilizers of the distal carpal row

Transverse stability of the distal carpal row is guaranteed by the flexor retinaculum and by strong intercarpal ligaments [2, 6]. Failure of these transverse structures results in splitting the wrist into two or three unstable columns (so-called "axial" instability) [25].

Carpal biomechanics

Although knowledge about the biomechanic characteristics of the wrist has grown rapidly during the last decades, many aspects of carpal function and dysfunction are still poorly understood.

Kinetics of carpal force transfer

The wrist must sustain not only the externally applied loadings, but also has to resist internal forces resulting from muscle contraction. The total of all forces is transmitted to the distal carpal row, and then distributed towards the proximal carpus. At the midcarpal level, about 60% of the load is transmitted across the scaphoid-lunate-capitate compartment; at the radiocarpal level about 50% of the load is present at the radius-scaphoid joint, 30% at the radius-lunate joint, and 20% at the ulnocarpal compartment [26].

The distal carpal row is considered as one functional unit due to the very tight ligamentous connections [5]. Because no tendon attaches the proximal carpal row, all axes of rotation are located at the distal carpal row, where rotational motions start first, later followed by movements of the proximal row [5]. Moderate carpal flexion-extension movements are feasible at the midcarpal joint.

Kinematics of the proximal carpal row

At the proximal carpal row, opposite torques are acting. Under axial load the scaphoid preferentially flexes, whereas the lunate, as well as the triquetrum, favors extension. The proximal carpals, which are less tightly bound to one another, show synergistic movement patterns, but each of them is differently mobile with regard to the degree of motion [5, 26].

Due to its narrow proximal curvature, the scaphoid is able to flex and extent about 30 degrees more intensively than the lunate [15]. Furthermore, the oblique alignement of the scaphoid causes a load transmission parallel to its longitudinal extension with two force vectors straightened out dorsally and proximally (Fig. 2). The dorsal force vector is resisted by the volar tilt of the radial scaphoid fossa. The proximal force vector is associated with an inherent flexion tendency of the scaphoid which is counteracted by the SLL as well as by the secondary stabilizers (STTL, RSCL) and the bowstringing of the FCR tendon [3].

The lunate—intercalated between the stable elements of the radius and capitate—is highly unstable due to minor ligamentous insertions only. Its functional position within the proximal row is determined mainly by the radiolunate and capitatolunate contact pressures proximally and distally, by the tension of the SLL and LTL laterally and medially, and by the contraction forces of the flexor and extensor muscles [3].

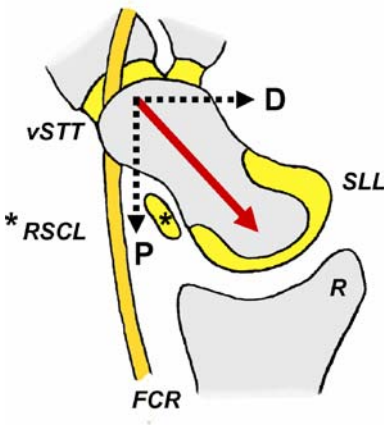

Fig. 2 Schematic diagram of the forces transmitted across the scaphoid. Under axial load a longitudinal force vector (in *red*) is initiated within the scaphoid. This obliquely orientated vector is built of two fractions, a dorsal (*D*) and a proximal (*P*) vector, respectively. The dorsal vector (*D*) is mainly counteracted by the geometry of the volarly tilted scaphoid fossa of the radius (*R*). The proximal force vector (*P*) would induce the scaphoid to flex, if not resisted by the primary (*SLL*) and secondary stabilizers (*vSTTL*, *RSCL*) of the scaphoid as well as the bowstringing of the FCR tendon. The RSCL is acting as the "volar support band" of the scaphoid

Multiangular kinematics of the wrist

Flexion and extension motion takes place in the radiocarpal as well as in the midcarpal joints in a nearly equiangular distribution. Maximal flexion is about 80 degrees and maximal extension about 85 degrees. Radial deviation is normally performable in about 25 degrees, ulnar deviation normally in about 40 degrees, each around an axis through the head of the capitate [5, 27]. However, the kinematics of radioulnar deviation is complex and multiangular, thereby combining several motion patterns in an individual way. For example, the entire proximal row is simultaneously flexed as the wrist is deviated radially, and extends smoothly during ulnar deviation [5, 12, 18]. The continuous out-of-plane mobility between the carpal rows is mainly controlled by the TCSL, the SCL and the dRLTL, all crossing and stabilizing the midcarpal joint [2].

In all wrist positions, the articular congruence between the forearm and the distal carpal row is maintained, and the carpal height is always constant. Therefore, the proximal carpal row is a flexible placeholder intercalated between the forearm and the stable distal carpal row.

Pathogenesis

Most instability patterns are caused by acute or repetitive injuries of the wrist. Hyperextension injuries commonly lead to ligamentary lesions on the radial side [28]. Fractures of radius or scaphoid can be associated. The infrequent hyperpronation injuries can cause instability patterns on the ulnar side [29]. Furthermore, posttraumatic sequela, like an abnormal articular tilt of a malunioned distal radius fracture, may consequently result in an instable wrist. Aside from traumatic causes, carpal instability can arise from other conditions and comorbidities, like avascular osteonecrosis [30], systemic inflammatory disease [i.e., calcium pyrophosphat hydroxylapatit deposition disease (CPPD) and rheumatoid arthritis] [31], neurological disorders (i.e., syringohydromyelia), and specific congenital malformations (i.e., Madelung's deformity).

Physical examination

A thorough investigation should include the mechanism of trauma, the type and intensity of complaints, inspection of

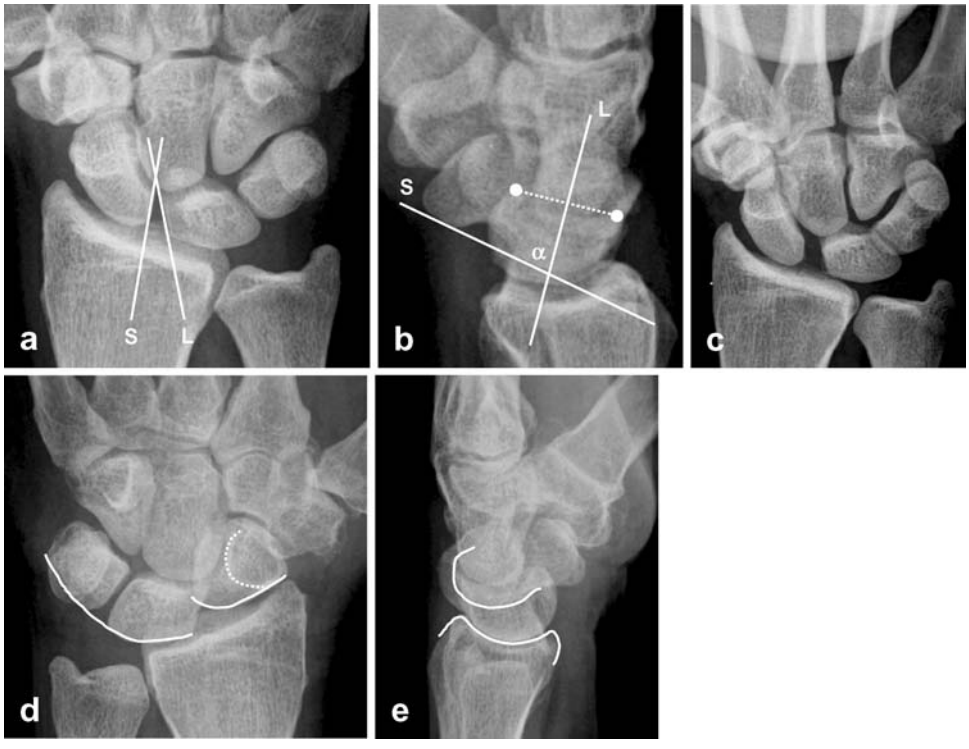

Fig. 3a–e Radiographic signs in stage III of SLD (two different cases). **a** The articulating joint surfaces of the scaphoid (*S*) and the lunate (*L*) are not arranged parallelly. **b** The scapholunate angle α in increased to 79 degrees. The angle α is between the line tangential to the volar border of the scaphoid (*S*) and the central line of the lunate (*L*) that is drawn perpendicularly to the connecting line between the anterior and posterior poles of the lunate. **c** The scapholunate gap is significantly widened up to 4.5 mm ("Terry Thomas sign") in the stress view attained during a forced grip. **d** The proximal carpal arc (Gilula's line I) is broken at the scapholunate junction. Furthermore, there is a "ring sign" of the distal scaphoid pole due to marked flexion. **e** In the lateral view, dorsal rotatory subluxation of the scaphoid is evident. The proximal scaphoid pole "rides" somehow on the dorsal rim of the distal radius joint. Articular contours are outlined

the skin and the presence of joint swelling, active and passive motions of the wrist, the palpation for focal tenderness, the testing of grip strength, and assessment of the neurovascular status. The careful clinical examination is imperative not only for ordering the exact imaging modality, but also for interpreting the radiographic findings correctly [32, 33].

Arthroscopy

In addition to the patient's history, physical examination and conventional radiograms, arthroscopy has emerged as the standard of reference for investigating wrist pain and carpal dysfunction [34]. The capability of arthroscopy to directly visualize the intraarticular structures, with the option of subsequently treating lesions endoscopically, has generally been accepted as advantageous. Yet, wrist arthroscopy is not only operator-dependent, but rather invasive when applied for diagnostic evaluation only.

Radiological techniques

The initial stages of carpal instability can be difficult to discern by radiological examinations. Dynamic instability is present if the carpal bones appear normal in standard X-rays, but an abnormal movement is identified in clinical examination, stress films or kinematography. Static instability is present, if the abnormal carpal arrangement is already visible in standard X-rays at rest.

Conventional radiograms (CR)

For correct film interpretation, it is obligatory that both the dorsovolar and lateral radiograms are exposed with a beam aligned at the radiocarpal joint and with the wrist in neutral position (half rotation between the supinated and pronated wrist) [35]. In the normal dorsovolar radiogram, three smooth and parallel arcs (Gilula's lines) can be drawn along the carpals [36]. Derangement is evident when one or two of the carpal lines appear interrupted with a stepoff (Figs. 3d, 6a) or the configuration of the lunate changes from trapezoidal to triangular or moon-shaped (Figs. 10a, 11b) [37]. In normal wrists, the radiolunate joint area covers more than 50% of the proximal lunate joint surface. The radiolunate contact is decreased in the presence of ulnar translocation instability (Fig. 8a,b).

On true lateral radiographs (Figs. 3b, 6b, 10b), the carpal alignement is determined by tracing lines parallel to the longitudinal extension of the radius, lunate, capitate and scaphoid and by measuring at least these angles [7, 38]: radiolunate (normal range 0±15 degrees), lunocapitate

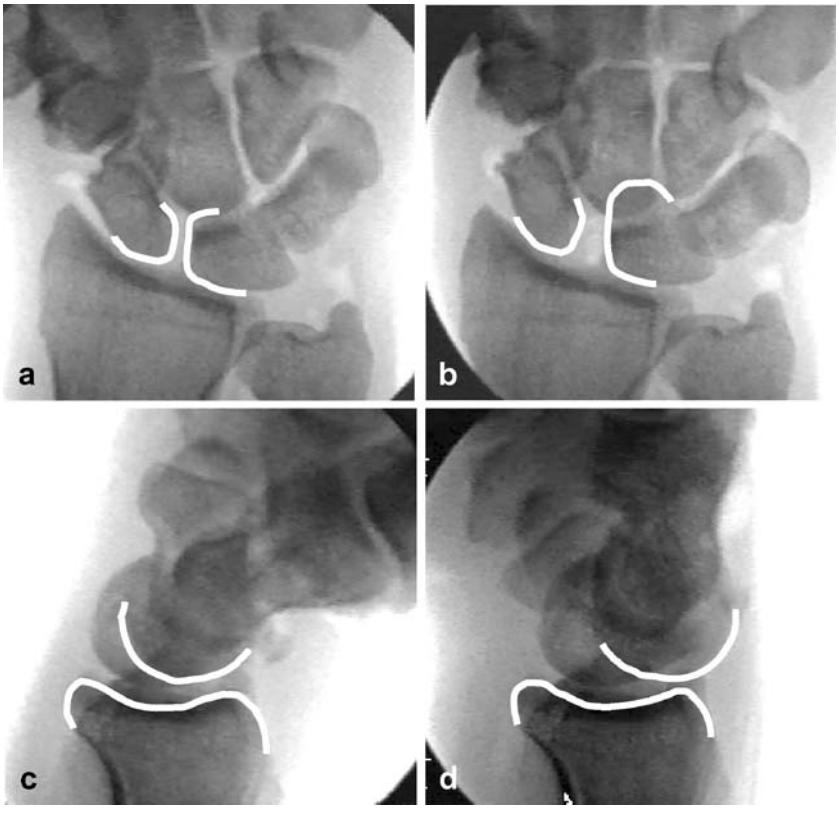

Fig. 4a–d Kinematography in dynamic scapholunate instability (stage II of SLD). Four snapshots are selected from a pulsed fluoroscopic examination using 15 images/s. **a, b** While progressively moving the wrist from radial deviation to ulnar deviation, the scapholunate gap suddenly widens to a distance of 5 mm (dorsovolar views). **c, d** During a progressive flexion-extension maneuver, the scaphoid abruptly volarflexes and dislocates dorsally to the RSS position (lateral views). Important contours are *outlined*

(normal range 0±15 degrees), and scapholunate (normal range 45±15 degrees). Every carpal angle exceeding these ranges must be considered as pathologic and suspicious of carpal instability. In the ideal wrist, the long axes of the radius, lunate, capitate and third metacarpal are colinear. The acronyms "DISI" and "VISI" describe two different derangements of the central column of the wrist, each presenting a zigzag deformity based on an abnormal rotation of the lunate as the intercalated and, thereby, potentially instable link [7]. A DISI configuration (dorsal intercalated segment instability) is present when the lunate is abnormally rotated in extension (Fig. 3b), whereas in the VISI configuration (volar intercalated segment instability) the lunate is abnormally rotated in flexion (Figs. 6b, 10b) [7].

Beside many others, two additional projections are recommended in carpal instability: the Stecher's view (fist clenched in ulnar deviation) and the 45-degree semipronated view [30].

Stress views (CR)

Even a severe ligamentary injury can be present without any diagnostic signs in standard radiograms. If an instable wrist is suspected, radiograms should be performed with the wrist under maximum loading. Traditionally, at least four stress projections are exposed: dorsovolar projections during the wrist in radial deviation and ulnar deviation as well as lateral projections during the wrist in flexion and extension [37, 39]. An unstable wrist can be documented efficiently on dorsovolar or volodorsal views with a clenched fist [40]. To the author's experience, the stress test is more fashionable while the patient's hand grips a tennis ball tightly (Fig. 3c). A refined modification is the "clenched pencil" view for exactly profiling the scapholunate gap [41]. In equivocal situations, comparison X-rays must be taken of the other hand.

Kinematography (CR)

Kinematographic examination is recommended if a motion-induced "click", "clunk" or "snap" phenomenon cannot adequately be explained with X-rays taken at rest and under stress loading [42, 43]. Different approaches are available: film kinematography (50 images/s), fluoroscopic videotaping (20–25 images/s), nonsubtracted DSA images (6–30 images/s), and digital documentation of pulsed fluoroscopy (15 frames/s). The projections in kinematography are similar to the stress views described above (Figs. 4, 11). Because the patient usually knows best which movement provokes a dynamic snap, the patient should be requested to actively perform the instability maneuver during kinematographic documentation.

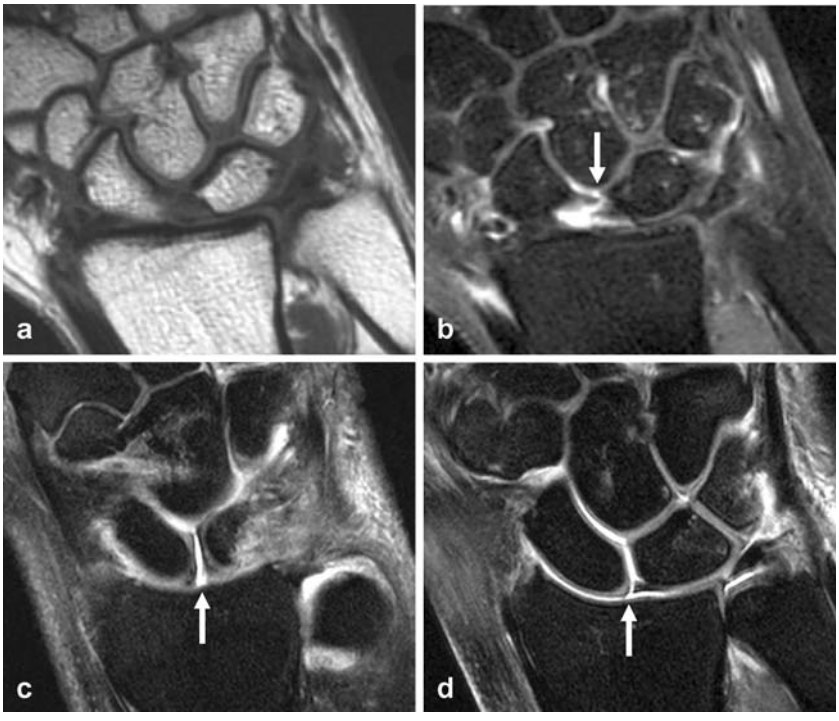

Fig. 5a–d Magnetic resonance imaging in two cases of SLD. **a** Plain and **b** contrast-enhanced T1-weighted SE images of a individual suffering from a complete SLL tear. Three minutes after intravenous application of the contrast agent, there is a focal synovial enhancement (*arrow*) at the rupture site enabling clear visualization of the ligament fragments (T1-weighted SE with fat-saturation). **c, d** MR arthrography in another case of complete disruption (*arrows*) of the SLL. The dorsal (**c**) as well as the volar (**d**) segments are dehiscent in the postarthrographic T1-weighted, fat-saturated SE images

Arthrography

The three-compartment arthrographic approach is recommended to precisely visualize uni- or bidirectional passages of the dye across ligamentary defect zones [44, 45]. In the classic technique, the contrast agent is firstly injected into the midcarpal and distal radioulnar joints under fluoroscopic control, followed by the arthrography of the radiocarpal joint two hours later. A modified procedure uses an adhesive marker-plate with radiopaque coordinates for simple puncture guidance [46]. Wrist arthrography enables the detection of communication defects with high sensitivity [45], but hampers from low specificity rates due to the inability to differentiate nonsymptomatic central defects from lesions of the peripheral ligament segments [44].

Mucoid degeneration of the carpal ligaments and the TFCC is a physiologic aging process that begins as early as the age of 30 years [44, 47]. Degenerative perforations are frequently found in the middle SLL and LTL segments. These central lesions do not alter the ligamentary strength nor cause instability, but may produce mild carpal discomfort. In mostly asymptomatic individuals, they sufficiently explain uni- or even bidirectional communication defects. In the elderly patient population, there is only a loose correlation between clinical and arthrographic findings [45, 48]. Therefore, it is recommened to combine wrist arthrography with a subsequent magnetic resonance imaging (MRI) or computed tomography (CT) examination [47, 49–52] to better assess the altered ligament segments (Figs. 5c,d, 6).

MRI

MRI carries the unique capability to directly visualize the carpal ligaments. Some methodical prerequisites must be considered. Firstly, scanners of at least 1.0- or 1.5-T field-strength are favorable for depicting the small structures of the wrist. The novel 3.0-T MRI machines have been proven to significantly increase the visibility of the carpal ligaments and the TFCC [53]. Secondly, the use of a multi-channel, phased-array surface coil is mandatory to create images of sufficient spatial and contrast resolution, respectively [54]. Thirdly, images in three orthogonal planes as well as different 2D sequences (T1-w SE, PD-/T2-w FSE, T2*-w GRE, STIR FSE) without and with fat-saturation must be acquired to obtain detailed information about the carpal malalignement and the altered ligaments [50–52]. For this reason, 3D-sequences (FLASH, MP-RAGE, VIBE, THRIVE) are reasonable. Finally, the application of intravenous or intraarticular contrast agent is discussed controversially in the literature.

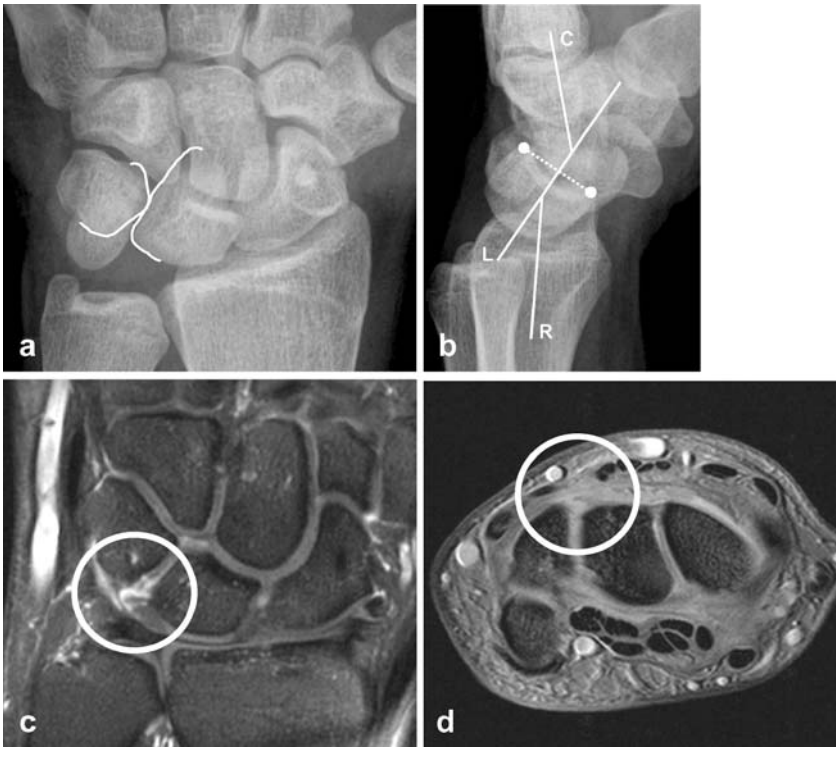

Fig. 6a–d Posttraumatic instability pattern of LTD in a patient suffering from pain and tenderness at the ulnar side of the wrist. **a** On the dorsovolar view, the lunate is not trapezoid, but moon-shaped. The lunotriquetral joint space is abnormal with nonparallel borders of the articulating partners (contours are *outlined*). **b** In the lateral view, a VISI (volar intercalated segment instability) configuration of the middle carpal column is present with increased radiolunate (*RL*) and capitatolunate (*CL*) angles over 15 degrees. **c** Contrast-enhanced MRI depicts the disruptured LTL (*circle*) due to focal hyperemia at the synovial and fibrovascular reparation tissue (T1-weighted SE sequence with fat-saturation). **d** The dorsal tear of the LTL (*circle*) is also visualized on the transaxial image of a plain T2*-weighted GRE sequence

Unenhanced MRI

In unenhanced MRI, the carpal ligaments are best seen in a T2*-weighted gradient-echo sequence [55] as well as in a fat-saturated proton-density-weighted sequence (Fig. 6d). Coronal slices should not be thicker than 2 mm to avoid partial-volume effects. Transaxial slices are recommended additionally, because they nicely depict the dorsal and volar ligament segments. Three-dimensional T2*-weighted gradient-recalled-echo sequences allow submillimeter imaging, and therefore they appear most useful to visualize the small-dimensioned SLL and LTL. Using this approach, diagnostic accuracy over 90% has been reported by some investigators [55, 56], but could not be verified by others [51]. Moreover, artifacts like the "magic-angle" effect are inherent with both sequence types in ligament imaging.

Contrast-enhanced MRI

In contrast-enhanced MRI, there is an increased gadolinium accumulation at the ruptured ligament, caused by hyperemia due to focal synovitis and fibrovascular tissue (Figs. 5a,b, 6c) [57]. The repairing process includes cellular, humoral and vascular reactions [58]. Although this approach has been used in clinical practice for several years, a study-proven significance of contrast-enhanced MRI for detecting tears of the carpal ligaments is still missing [57, 59].

Indirect MR arthrography

In indirect MR arthrography, active joint movement induces an intraarticular diffusion of the previously applied contrast agent, thus yielding an improved contrast ratio in T1-weighted sequences [59, 60]. However, the distending effect of the intraarticular structures obtained with indirect MR arthrography is only slight.

Direct MR arthrography

In direct MR arthrography, a 1:200 mixture containing gadolinium and X-ray dye is applied in a single- or multicompartment approach under fluoroscopic control followed by high-resolution 2D or 3D MRI (Fig. 5c,d) [61]. All intraarticular and intracapsular ligaments get distended, and the contrast level at the ligament-dye borders is significantly increased allowing precise identification of subtle ligamentary lesions [50]. In prospective studies using arthroscopy as the standard of reference, accuracy rates of about 95% have been reported for MR arthrography [51, 52].

Real-time MRI

Real-time MRI of the wrist movement is feasible with the use of high-field MRI scanners [62]. However, the carpal ligaments are not sufficiently depicted with dynamic MRI due to both reduced matrix size and limited acquisition speed. Currently, dynamic MRI offers no additional information compared to X-ray kinematography.

Computed tomography (CT)

Using multi-slice CT imaging, high-resolution 3D images can be acquired for detecting wrist fractures or articular lesions like subchondral sclerosis and cysts. CT imaging should be performed in equivocal cases to confirm or rule out an early onset of carpal osteoarthritis in the treatment planning of carpal instability [63].

Ultrasound (US)

High-resolution US has been applied for evaluating the intrinsic and the extrinsic carpal ligaments. Rates of detectability were found in ranges from 0% for the RSLL, over 61% and 62% for the dorsal LTL segment and the RSCL, respectively, and up to 93% and 97% for the dRLTL and the dorsal SLL segment, respectively [64]. The volar and middle SLL segments are often hidden for US detection [65, 66]. In the presence of SLD, the normal hyperechoic fibrillar ligament is hypoechoic or absent [67, 68]. However, the diagnostic value of US is controversially discussed. In the presence of a visible SLL, US is judged to be helpful to exclude SLD, but its absence on US does not necessarily indicate a tear [66]. Moreover, in comparison to arthroscopy false-negative US results were found in dynamic SLD leading to decreased sensitivity of US [69]. Finally, US is not accurate for the evaluation of lunotriquetral tears, mainly due to the small size of the LTL [65]. In conclusion, high-resolution US is an emerging procedure; however, currently it should only be used in carpal instability as an adjunct to other diagnostic modalities.

Classification

The Mayo Clinic classification [34, 70] is mostly used to describe the different patterns of carpal instability (Table 2). In this classification, the differentiation of so-called "dissociative" instabilities from "non-dissociative" instabilities is essential. The functional continuity of the proximal carpal row is evaluated for this reason [70, 71]. In the dissociative group [carpal instability dissociative

(CID)], the elements of the proximal carpal row are malaligned, either during motion ("dynamic") or at rest ("static"). In the nondissociative group [carpal instability nondissociative (CIND)], the proximal carpal row remains intact, but is dynamically or structurally malaligned with the distal row. In these cases, the entire unit of the proximal row subluxates volarly or dorsally with respect to the distal row, or migrates ulnarly in relation to the forearm (ulnar translocation). Two further instability subcategories will not be further elucidated in this review paper, the complex instability group with features of both dissociative and nondissociative types [carpal instability complex (CIC)], and finally the axial instability group that is almost always combined with fracture dislocations of the wrist [25, 28].

Instability patterns

Dissociative instability group

This instability group includes the scapholunate and the lunotriquetral dissociation, and less frequently unstable scaphoid nonunion as well as Kienboeck's disease stage IIIb and IV.

Scapholunate dissociation (SLD)

This most important instability pattern may appear as an isolated injury or associated with a distal radius or scaphoid fracture, respectively. In addition to swelling, point tenderness over the anatomical snuff box and reduced movement, the Watson's scaphoid shift test [33] is sensitive for the presence of SLD (the examiner provokes a dorsal subluxation of the scaphoid). The rupture site of the ligament is most commonly on the scaphoid because Sharpey's fibers are less dense here. The spectrum of presentation is broad [17, 72, 73] and can be determined by different stages (Table 3).

Detection and staging of SLD using X-rays: In stage I ("predynamic" SLD), there is a partial lesion of the SLL, mostly at the volar and middle SLL segments [4]. Focal synovitis is caused by a minimal scapholunate hypermobility. There is no carpal malalignment present on standard X-rays, and the Watson's shift test, as well as kinematography, remains unremarkable.

In stage II ("dynamic" SLD), the SLL is completely disruptured; however, the stabilizing extrinsic ligaments remain intact [17, 72]. In most cases, standard radiograms reveal an unremarkable carpal alignment. An early, but infrequent sign in stage II can be the lack of parallel joint surfaces between the scaphoid and lunate in the dorsovolar radiogram (Fig. 3a) [37]. Stress views (Fig. 3c) or kinematography (Fig. 4a-d) should be performed when there are complaints suggestive for early SLD and the Watson's scaphoid shift test is positive. In kinematography, transitional changes of the carpal arrangement become visible [4, 72]: an abrupt, short widening of the scapholunate joint space is seen on the dorsovolar cinematogram during movement from radialduction to ulnarduction (Fig. 4a,b), and the dorsal rotatory subluxation of the scaphoid is identified on the lateral kinematogram, while the wrist moves from the extented to the flexed position (Fig. 4c,d).

In stage III ("static" SLD), a complete tear of the SLL as well as lesions of the secondary stabilizers are manifest [17]. According to Lichtman's "model of the carpal ring" [30], any complete loss of ligamentary fixation allows the scaphoid and lunate bones to move independently and freely according to their natural tendency. Now, the survey radiograms show the unstable scapholunate articulation with opposite rotations of the scaphoid and the lunate (Fig. 3a). The scaphoid rotates into a marked flexion, and is simultaneously pressed onto the dorsal crest of the radius [4, 72]. This motion pattern is referred to as "rotation subluxation of the scaphoid" (RSS) [73]. On the lateral radiogram, the flexed scaphoid "rides" on the dorsal rim of the radius (Fig. 3e), while on the dorsovolar view the scaphoid appears shortened and forms the so-called "ring sign" (Fig. 3d). The unconstrained lunate rotates dorsally owing to its wegde-shaped configuration [12] and under the influence of the triquetrum as well (Fig. 3b) [13]. Additionally, the lunate moves into a mild volar

Table 2 Classification of carpal instability in the modified classification of Amadio [30])

Instability group	Instability entity	Pathoanatomic cause
Dissociative	Scapholunate dissociation	Tear of the SL ligament (and secondary stabilizers)
	Lunotriquetral dissociation	Tear of the LT ligament (and secondary stabilizers)
Nondissociative	Radiocarpal instability	Tears of the RSC, vRLT and dRLT ligaments, secondary to malunioned radius fracture
	Midcarpal instability	Congenital weakening or tears of the TCS and dIC ligaments
Complex	Perilunate	Carpal dislocation around the lesser arc
	Transscaphoid perilunate	Fracture dislocation around the greater arc
Transaxial	Radial	Axial injury at the radial wrist
	Ulnar	Axial injury at the ulnar wrist
	Radial and ulnar	Axial injury at both the radial and ulnar wrist

Table 3 The stages of scapholunate instability (scapholunate dissociation) in the modified classification of Watson et al. [33]

Stage	Description	Ligamentary status	Carpal function
I	Pre-dynamic	Partial tear of the SL ligament	Normal at rest, normal under load
II	Dynamic	Complete tear of the SL ligament	Normal at rest, SL instability under load
III	Static	Complete tears of the SL ligament and the secondary stabilizers	SL instability at rest
IV	Osteoarthrotic	Complete tears of the SL ligament and the secondary stabilizers	Osteoarthritis secondary to SLD

position, raising a midcarpal subluxation of the capitate at the posterior horn of the lunate. The zigzag deformity that develops in the middle carpal column is called the "dorsiflexed intercalated segment instability" (DISI) [7]. As the consequence , the scapholunate angle is increased to over 60° on the lateral radiogram, what is the most evident sign of SLD (Fig. 3b). On the dorsovolar view, the extended lunate no longer appears trapezoid, but triangular with projection of its anterior pole onto the capitate (Fig. 3a). The scapholunate gap may be increased to over 3 mm, the optional "Terry-Thomas sign" (Fig. 3c), which is not always present in SLD.

It might be reasonable to add stage IV ("osteoarthrotic" SLD) to the classification system when typical findings of osteoarthritis are visible on X-rays. Degenerative changes begin at the radiocarpal joint between the proximal scaphoid pole and the dorsal rim of the radius [74]. The osteoarthritis progresses to the entire radioscaphoid compartment and reaches the midcarpal joint at the scapho- and lunocapitate articulations finally. Now, the capitate migrates into the scapholunate gap and approaches the radius, leading to the "scapholunate advanced collapse" (SLAC wrist) [74]. The height of the carpus is significantly reduced, measured with the Youm Index (length ratio of the carpus and the third metacarpal, respectively; normal is 0.54±0.03).

Conventional arthrography is a poor predictor of SLD, because unilateral or even bilateral communication defects are detectable also in the presence of degenerative lesions of the middle SLL segment seen physiologically in asymptomatic individuals [44].

Diagnosis of SLD using MRI: MRI allows visualization of the radiologically "silent" instability stages I and II of SLD. A ligament insufficiency must be assumed when at least the dorsal SLL segment or all SLL segments are dehiscent, whereas a focal defect of the middle or volar SLL segment is not significant for instability.

In T2-weighted sequences, the torn SLL is identified by a hyperintense fluid accumulation adjacent to the ligamentary flaps or in case of an absent ligament. Coronal as well as transaxial slices are mandatory to fully visualize the altered SLL. Accuracy rates of plain MRI have been reported in ranges between 50 and 80% [55, 56].

In SLL and other ligamentary tears, there is an enhancement of gadolinium at the rupture site, caused by an intense hyperemia of synovial and fibrovascular tissue (Fig. 5a,b). This regeneration process develops focally at the tear immediately after the injury and is seen in contrast-enhanced MRI up to 9 months. Obviously, the application of intraveneous contrast agent increases the accuracy of MRI [57], but the study-based significance of contrast-enhanced MRI for detecting tears of the carpal ligaments is still missing.

The ruptured SLL can be identified most precisely with MR arthrography. By directly applying the contrast agent into the carpal joints, the SLL segments are clearly depictable, thus partial tears can be differentiated from complete tears (Fig. 5c,d). Furthermore, anatomic details like the rupture site and flaps as well as the retracted and thickened ligament get visible (Fig. 9). MR arthrography has an accuracy rate of over 95% for diagnosing the ruptured SLL [51, 52, 61].

Actually, there is no report dealing with the MRI diagnostics of the secondary scapholunate stabilzers [2, 17].

Lunotriquetral dissociation (LTD)

LTD is rare. Usually, an isolated rupture of the LTL causes no symptoms. The adjacent extrinsic ligaments (vRLTL, UTL and dRLTL) must also be injured to produce complete lunotriquetral instability with pain at the ulnar side of the wrist and a motion-associated click phenomenon. The coincidence with TFCC lesions is frequent (classes II D and II E in Palmer's classification) [75]. Typical for LTD is the increased flexion of the lunate together with a slight dorsal translation, caused by the flexion tendency of the scaphoid, which is coupled to the lunate via the intact SLL. This volar zigzag deformity of the middle carpal column is called the "volarflexed intercalated segment instability" (VISI) [18]. The triquetrum remains linked to the hamate [7, 18].

Detection and staging of LTD using X-rays: The classification scheme suggested for SLD is recommended for LTD, too. In stage I ("pre-dynamic" LTD), a partial LTL tear is silent in symptoms and X-ray diagnostics. In stage II ("dynamic" LTD), the LTL is completely ruptured, but the extrinsic ligaments remain intact. Standard radiograms are unremarkable, and the tear can only be identified kinematographically by means of opposite rotational movements of the scaphoid-lunate block and the triquetrum. In stage III ("static" LTD), signs of VISI

instability become visible in standard X-rays (Fig. 6a,b). Both the scaphoid and lunate bones are in volar flexion, while the triquetrum is extended. On the dorsovolar view, the lunate is typical moon-shaped with projection of the posterior horn onto the capitate [37]. Further characteristics are the deformed carpal arcs I and II (Gilula) at the lunotriquetral level, and sometimes a displaced lunotriquetral/capitatohamate junction. The triquetrum is in a "low" position near the distal pole of the hamate. In stage IV ("osteoarthrotic" LTD), signs of articular degeneration are manifest in the midcarpal joint.

Diagnosis of LTD using MRI: Due to its small size, direct MRI visualization of the LTL is challenging. LTD must be assumed when either the volar or the dorsal LTL segments or both appear dehiscent. Central lesions are of no biomechanical importance; however, they can cause focal synovitis and may therefore be painful. Plain MRI has an accuracy of only about 50% in the diagnosis of a ruptured LTL. An accumulation of fluid can be present at the rupture site in T2-weighted sequences. The LTL should also be evaluated in transaxial, T2*-weighted images (Fig. 6d). Contrast-enhanced MRI significantly increases the visibility of a ruptured LTL [57]. A focal gadolinium enhancement is seen at the acutely or subacutely injured LTL (Fig. 6c). A better description of the rupture site can be achieved with high-resolution CT arthrography (Fig. 7) and with MR arthrography. However, an accuracy rate of about 80% even in MR arthrography is not satisfactory [51, 52].

Nondissociative instability group

Nondissociative carpal instabilities (CIND) are characterized by articular dysfunction either between the forearm and the proximal carpal row (radiocarpal CIND) or between the proximal and distal rows (midcarpal CIND), while the articular function is preserved within each row [70, 71].

Fig. 7 Traumatic disruption of the LTL associated with fractures of the distal forearm. Aside a Chauffeur's fracture of the radius and an avulsion lesion of the ulnar styloid process, CT arthrography synoptically show tears of the LTL (*arrow*) and of the triangular fibrocartilage which is retracted ulnarly. The SLL is uneffected

Radiocarpal instability

Under physiologic conditions, the obliquely running "slingshot" ligaments (vRLTL, RSCL, dRLTL) resist the tendency of the carpus to slide down on the articular tilt of the radius. Any failure of these controlling forces is likely to result in an ulnar and volar translocation shift of the carpus leading to deformity and dysfunction of the wrist [23, 24]. Madelung's deformity and rheumatoid arthritis are the most frequent causes, whereas traumatic radiocarpal dislocation is considered rare [31]. Furthermore, radiocarpal instability can have an iatrogenic origin; i.e., excessive resection of the radial styloid process or of the ulna head, respectively [7].

Ulnar translocation: Ulnar translocation of the wrist may have two different presentations, which must be differentiated in treatment planning [76]. If the entire carpus slips to the ulnar side (Taleisnik type I), a true CIND instability is present. Now, a radioscaphoid diastasis of more than 2 mm opens up, while the radiolunate contact is less than 50% (Fig. 8a,b) [37]. In case of intact RSCL and RSL, the scaphoid bone remains in place, while the lunate-triquetrum block is displaced towards the ulnar side, causing a scapholunate diastasis (Taleisnik type II). This feature is a combined CIND and CID pattern, also referred as to CIC instability ("carpal instability complex") [62]. Radiocarpal osteoarthritis as well as an ulnocarpal neoarticulation process will develop early.

Other translocation patterns: Other radiocarpal CIND instability patterns are quite rare. Three subcategories must be defined [70]. Firstly, volar translocation of the wrist can follow a traumatic disruption of only the radiocarpal ligaments [77] or is of inflammatory origin in rheumatoid arthritis and CPPD arthropathy [31]. Secondly, a radial translocation can occur in case of a longstanding scaphoid nonunion (Fig. 8d), when the proximal fragment is significantly reduced in size and the ulnocarpal ligaments (UTL, ULL) are insufficient for counteracting the radial shift. Thirdly, radiocarpal dislocations can be associated with displaced or badly malunited fractures of the distal radius [77, 78]. Particularly, impacted fractures of the radial styloid process (type Chauffeur, Fig. 8c) and the dorsal rim (type Barton) can induce severe dislocations of the entire wrist. Most often, a dorsal tilt of the joint surface causes the entire proximal carpal row to rotate into extension (DISI pattern). For compensation the distal carpal row shifts into a flexed position. However, a normal (Fig. 9a,b) or even a VISI alignement of the proximal row

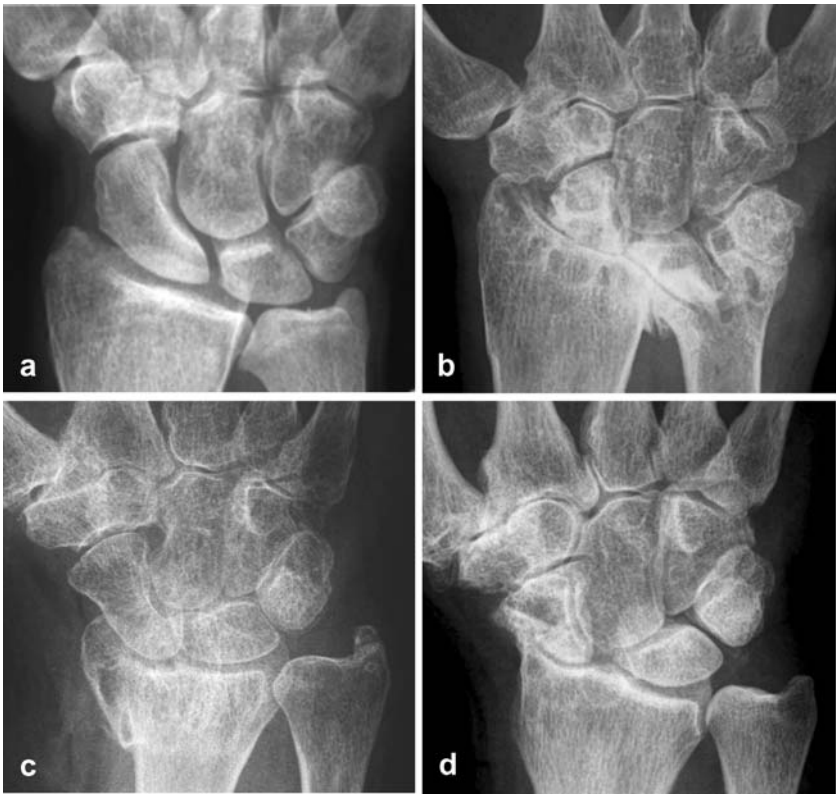

Fig. 8a–d The different patterns of radiocarpal translocation instability. **a** Ulnar translocation of the wrist (Taleisnik's type I) following traumatic disruption of the radiocarpal "slingshot" ligaments. Please, note the widened radioscaphoid joint as well as the decreased radiolunate contact length. **b** Ulnar translocation of the wrist (Taleisnik's type I) caused by long-standing chondrocalcinosis (CPPD deposition disease). Advanced osteoarthrotic and cystic changes are present around the radiocarpal joint. **c** Radial translocation of the wrist as a sequel of a malunited Chauffeur's fracture of the radius. The ulnar inclination of the radius is pathologically reduced, and the radiolunate contact diameter is increased. **d** Radial translocation of the wrist in the advanced stage of SLD associated with a collapse of the wrist and osteoarthritis of the radiocarpal and midcarpal joints (SLAC wrist)

can also be found. One should keep in mind that a dislocation pattern caused by a radial fracture is—by definition—not a "true" CIND instability because the carpal malalignement is secondarily induced by a lesion outside the wrist [8]. This "re-balanced" arrangement is also referred as to "carpal instability adaptive" (CIA).

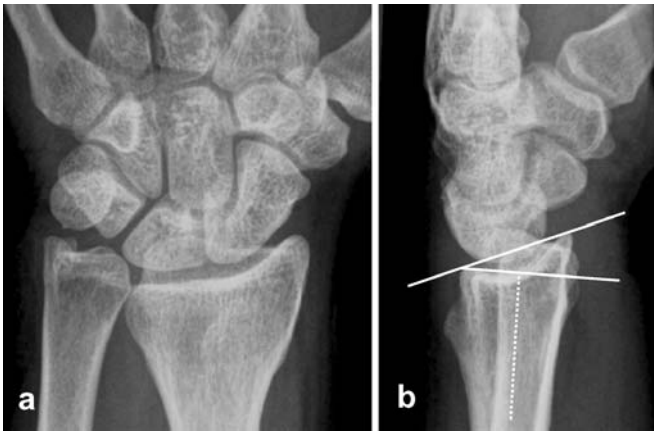

Fig. 9a, b Carpal instability caused by a malunited Colles' fracture of the distal radius. There is a dorsal tilt of the radial joint surface of about 26 degrees that results from a significant impaction of the dorsal radial fragment. Indeed, the entire wrist is translocated dorsally, but the proximal carpal row is not significantly tilted

Midcarpal instability (MCI)

The abnormal mobility of the proximal carpal row is the diagnostic sign of the "intrinsic" MCI pattern [7, 71]. At rest, the proximal carpal row is either still in a normal position (dynamic MCI) or is flexed (static MCI). In the presence of MCI, the nondissociative VISI deformity is the posture of preference under axial load. Additionally, both

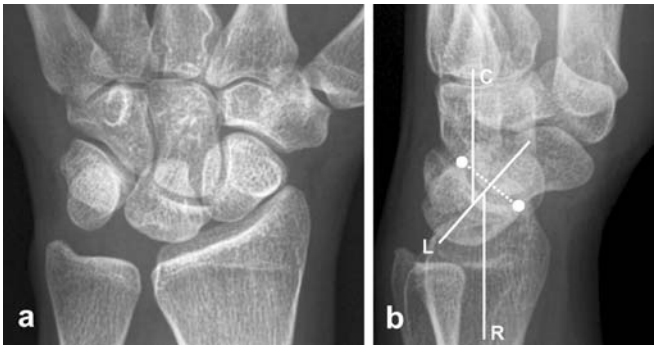

Fig. 10 Static midcarpal instability (Lichtman's type I). At rest, the entire proximal carpal row appears abnormally flexed. This nondissociative VISI pattern causes the positive "ring sign" and the moonlike shape of the lunate in the dorsovolar radiogram. The alignement of the radius-lunate-capitate chain is no further colinear leading to increased radiolunate (*RL*) and capitatolunate (*CL*) angles as assessed in the lateral view. However, the scapholunate and lunotriquetral angles are in normal ranges

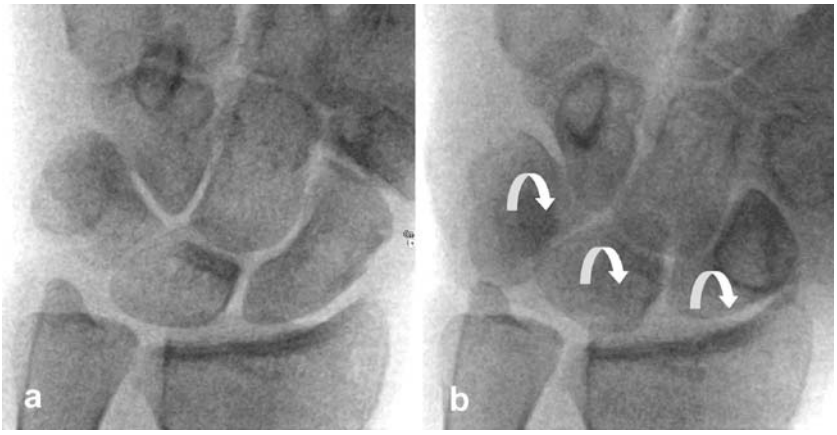

Fig. 11a, b Kinematography in dynamic midcarpal instability. Two snapshots are displayed from a pulsed fluoroscopic scene (15 images/s). While progressively moving the wrist from ulnar deviation to radial deviation, the entire proximal carpal row remains iniatially in an extended position (**a**), before it suddenly "jumps" into a flexed rotation (**b**) accompanied by a painful click. The curved arrows indicate the typical signs of flexion (ring sign of the scaphoid, moon-shape of the lunate, low position of the triquetrum)

carpal rows are not able to rotate smoothly from flexion to extension; however, there is a "snapping" motion pattern caused by a transient en-bloc rotation of the proximal row opposite towards the distal row [7, 79]. During radial deviation the proximal carpal row "jumps" abruptly into a flexed position; and vice versa into sudden extension as the wrist deviates ulnarly. Patients suffering from MCI usually complain about a painful clunk and a reduced grip strength.

The pathomechanism for MCI still remains controversial. It may include an inadequate ligamentary control within the midcarpal joint, particularly in the hamatotriquetral compartment [12]. Congenital or acquired weakness of the midcarpal stabilizers (TCSL, SCL, dRLTL) is assumed for causing the MCI [2, 71, 79, 80].

Four different subcategories of MCI have been described [71, 79, 80], thereby differentiating static and dynamic instability patterns as well as nondissociative VISI and DISI, respectively (Table 4). The so-called CLIP instability (capitatolunate instability pattern) is a dynamic MCI that is exclusively localized at the capitatolunate compartment, here yielding a focal dislocation during motion [80].

Diagnosis of MCI using X-rays: In static MCI, X-rays show the signs of VISI malalignment in the dorsovolar views (foreshortened scaphoid, moonlike lunate, unaltered Gilula's lines, see Fig. 10a) and lateral views (both radiolunate and capitatolunate angles being increased, see Fig. 10b), or a DISI malalignment in case of a severely malunited radius fracture; however, standard radiograms are nondiagnostic in the presence of a dynamic MCI pattern. Kinematography is the procedure of choice to document the nonsynchronized carpal movement [43]. As the wrist deviates radially, the proximal carpal row remains iniatially in a flexed position, followed by a jump-like rotation synchronously with a painful click on the ulnar side of the wrist (Figs. 11a,b). The CLIP instability is confirmed when the capitatolunate dislocation of at least half the width of the capitate head can be provoked by applying a dorsovolar displacement load under fluoroscopic control [80].

Diagnosis of MCI using MRI: No MRI report is available about this topic in the recent literature. Probably, MRI allows direct visualization of the insufficient ligaments. In constitutional midcarpal instability, the TCSL should either be missing or hypoplastic, whereas tears of the TCSL and the dRLTL should be detectable by means of contrast-enhanced MRI.

Table 4 The four subcategories of midcarpal instability (MCI) in the classification of Lichtman et al. [79]

MCI pattern	Alignment of the proximal carpal row	Altered ligaments
Volar	Nondissociative VISI at rest	Volar midcarpal ligaments (TCSL, STTL, SCL) attenuated or disruptured
Dorsal	Normal alignment at rest, nondissociative DISI under loading	Volar support ligament (RSCL) attenuated or disruptured
Dorsal and volar	Either nondissociative VISI or DISI at rest	Lax radiocarpal and midcarpal ligaments
Extrinsic	Mostly, nondissociative DISI at rest (VISI also possible)	Stretched RSCL and UCL caused by malunited radius fracture

MCI (CIND-VISI) and LTD (CID-VISI) may be indistinguishable in standard radiograms. However, examination maneuvers like the ballottement and shear tests [22], and the use of kinematography, arthrography and MRI, almost always enable differentiation of these ulnarsided instability patterns.

Discussion

Carpal instability is a sophisticated diagnostic topic with several challenges for the radiologist. Mainly, the initial stages of carpal instability are difficult to discern, when signs in X-ray are completely missing or subtle; i.e., slightly nonparallel articular contours.

Based on this short review, we would like to recommend a diagnostic algorithm as follows. (1) If the radiograms appear predominantly inconspicuous in a patient suffering from carpal dysfunction, then particular care must be provided for analysis of the Gilula's lines [36] and the carpal angles [37]. (2) In the presence of carpal instability, but normal X-ray findings, the next step in diagnostic imaging should be a kinematographic study [42, 43]. Using pulsed fluoroscopy and PACS documentation, the movement analysis of carpal dysfunction, as well as the interdisciplinary communication, is significantly facilitated. (3) Although not frequently used in the diagnosis of carpal dysfunctions, MRI appears an ideal tool for the comprehensive assessment of the ligamentary lesions underlying the suspected instability pattern. Direct MR arthrography, which is only minimal invasive, is most reliable to detect lesions of the intrinsic ligaments. With the use of intravenous or intraarticular contrast agent, high-resolution MRI can provide detailed visualization not only of the intraarticular ligaments [51, 52, 54] but also of the extraarticular soft-tissues [50, 55], the latter not being completely depictable with arthroscopy.

Further research efforts must be encouraged to fully incorporate US and MRI into the diagnostic sequela of carpal instability, side-by-side with invasive arthroscopy. Currently, the secondary ligamentary stabilizers of the scaphoid as well as the midcarpal stabilizers are of particular diagnostic and therapeutic interest [17]. In future, these subtle carpal ligaments will probably be attainable for direct visualization with the dedicated use of MRI and US; especially US has an emerging role for this purpose [64].

Carpal instability nearly always goes along with adverse social consequences both in terms of disability and morbidity if inadequately treated or even not detected [74]. Therefore, the radiologist must be aware of this challenge with regard to early and precise diagnosis of carpal instability as an important, but frequently not enough appreciated entity of the musculoskeletal system.

Acknowledgement We are grateful to Dr. Claudia Lipke, University of Regensburg, for critical proofreading of the manuscript.

References

1. Kauer JMG (1986) The mechanism of the carpal joint. Clin Orthop 202:16–26
2. Garcia-Elias M (1997) Kinetic analysis of carpal stability during grip. Hand Clin 13:151–158
3. Dobyns JH, Linscheid RL (2004) A fifty-year overview of wrist instability. In: Berger RA, Weiss AP (eds). Hand surgery, vol. 1. Lippincott, Williams and Wilkins. Philadephia, pp 461–479
4. Kobayashi M, Berger RA (1995) Kinematic analysis of scapholunate interosseous ligament repair. Orthop Trans 19:129
5. Ruby LK, Cooney WP III, An KN, Linscheid RL, Chao EY (1988) Relative motion of selected carpal bones: a kinematic analysis of the normal wrist. J Hand Surg 13A:1–10
6. Taleisnik J (1976) The ligaments of the wrist. J Hand Surg 1A:110–118
7. Linscheid RL, Dobyns JH, Beabout JW, Bryan RS (1972) Traumatic instability of the wrist: diagnosis, classification and pathomechanics. J Bone Joint Surg 54A:1612–1632
8. Anatomy and Biomechanics Committee of the IFSSH (1999) Position statement: definition of carpal instability. J Hand Surg 24A:866–867
9. DiBenedetto MR, Lubbers LM, Ruff ME, Nappi JF, Coleman CR (1991) Quantification of error in measurement of radial inclination angle and radial-carpal distance. J Hand Surg 16A: 399–400
10. Linscheid RL (1986) Kinematic considerations of the wrist. Clin Orthop 202:27–39
11. Boabighi A, Kuhlmann JN, Guerin-Surville H (1988) A new radiological approach to the radiocarpal joint: modified lateral projection of the wrist. J Radiol 69:465–467
12. Kauer JMG (1974) The interdependence of articulation chains. Acta Anat 88:481–501
13. Weber ER (1984) Concepts govering the rotational shift of the intercalated segment of the carpus. Orthop Clin North Am 15:193–207
14. Feipel V, Rooze M (1999) The capsular ligaments of the wrist: morphology, morphometry and clinical applications. Surg Radiol Anat 21:175–180
15. Berger RA, Imeada T, Berglund L, An KN (1999) Constraint and material properties of the subregions of the scapholunate interosseous ligament. J Hand Surg 24A:953–962
16. Sokolow C, Saffar P (2001) Anatomy and histology of the scapholunate ligament. Hand Clin 17:77–81
17. Short WH, Werner FW, Green JK, Masaoka S (2002) Biomechanical evaluation of ligamentous stabilizers of the scaphoid and lunate. J Hand Surg 27A:991–1002

18. Horii E, Garcia-Elias M, An KN, Bischop AT, Cooney WP, Linscheid RL, Chao EY (1991) A kinematic study of lunotriquetral dissociations. J Hand Surg 16A:355–362
19. Watson K, Ottoni L, Pitts EC, Handal AG (1993) Rotary subluxation of the scaphoid: a spectrum of instability. J Hand Surg 18B:62–64
20. Berger RA, Kauer JMG, Landsmeer (1991) Radioscapholunate ligament: a gross anatomic and histologic study of the fetal and adult wrist. J Hand Surg 16A:350–355
21. Berger RA, Landsmeer JMF (1990) The palmar radiocarpal ligaments: a study of adult and fetal human wrist joints. J Hand Surg 15A:847–854
22. Ambrose L, Posner MA (1992) Lunatetriquetral and midcarpal joint instability. Hand Clin 8:653–668
23. Rayhack JM, Linscheid RL, Dobyns JH, Smith JH (1987) Posttraumatic ulnar translation of the carpus. J Hand Surg 12A:180–189
24. Viegas SF, Patterson RM, Ward K (1995) Extrinsic wrist ligaments in the pathomechanics of ulnar translation instability. J Hand Surg 20A:312–318
25. Garcia-Elias M, Dobyns JH, Cooney WP III, Linscheid RL (1989) Traumatic axial dislocations of the carpus. J Hand Surg 14A:446–457
26. Hara T, Horii E, An KN, Cooney WP, Linscheid RL, Chao EY (1992) Force distribution across the wrist joint: application of pressure-sensitive conductive rubber. J Hand Surg 17A:504–508
27. Wolfe SW, Neu CP, Crisco JJ III (2000) In vivo scaphoid, lunate and capitate kinematics in wrist flexion and extension. J Hand Surg 25A:860–869
28. Mayfield JK, Johnson RP, Kilcoyne RK (1980) Carpal dislocations: pathomechanics and progressive perilunar instability. J Hand Surg 5A:226–241
29. Viegas SF, Patterson RM, Peterson PD, Pogue DJ, Jenkins DK, Sweo TD, Hokanson JA (1990) Ulnar-sided perilunate instability: an anatomic and biomechanic study. J Hand Surg 15A:268–278
30. Lichtman DM, Martin RA (1988) Introduction to the carpal instabilities. In: Lichtman DM (ed) The wrist and its disorders. Saunders, Philadelphia, pp 244–250
31. Resnick D, Niwayama G (1977) Carpal instability in rheumatoid arthritis and calcium pyrophosphate deposition disease. Ann Rheum Dis 36:311–318
32. Beckenbaugh RD (1984) Accurate evaluation and management of the painful wrist following injury: an approach to carpal instability. Orthop Clin North Am 15:289–306
33. Watson HK, Ashmead D IV, Makhlouf MV (1988) Examination of the scaphoid. J Hand Surg 13A:657–660
34. Cooney WP, Dobyns JH, Linscheid RL (1990) Arthroscopy of the wrist: anatomy and classification of carpal instability. Arthroscopy 6:133–140
35. Hardy DC, Totty WG, Reinus WR, Gilula LA (1987) Posteroanterior wrist radiography: importance of arm positioning. J Hand Surg 12A:504–508
36. Gilula LA (1979) Carpal injuries: analytic approach and case exercises. AJR Am J Roentgenol 133:503–517
37. Linn MR, Mann FA, Gilula LA (1990) Imaging the symptomatic wrist. Orthop Clin North Am 21:515–543
38. Larsen CF, Mathiesen FK, Lindequist S (1991) Measurements of carpal bone angles on lateral wrist radiographs. J Hand Surg 16A:693–888
39. Truong NP, Mann FA, Gilula LA, Kang SW (1994) Wrist instability series: increased yield with clinical-radiologic screening criteria. Radiology 192:481–484
40. Dobyns JH, Linscheid RL, Chao EYS (1975) Traumatic instability of the wrist. Instr Course Lect 24:189–199
41. Lawand A, Foulkes GD (2003) The "clenched pencil" view: a modified clenched fist scapholunate stress view. J Hand Surg 28A:414–418
42. Nielsen PT, Hedeboe J (1984) Posttraumatic scapholunate dissociation detected by wrist cineradiography. J Hand Surg 9A:135–138
43. Protas JM, Jackson WT (1980) Evaluating carpal instabilities with fluoroscopy. AJR Am J Roentgenol 135:137–140
44. Metz VM, Mann FA, Gilula LA (1993) Three-compartment wrist arthrography: correlation of pain site with location of uni- and bidirectional communications. AJR Am J Roentgenol 160:819–822
45. Linkous MD, Pierce SD, Gilula LA (2000) Scapholunate ligamentous communicating defects in symptomatic and asymptomatic wrists: characteristics. Radiology 216:846–850
46. Berna-Serna JD, Martinez F, Reus M, Alonso J, Domenech-Ratto G (2006) Wrist arthrography: a simple method. Eur Radiol 16:469–472
47. Cerezal L, Abascal F, Garcia-Valtuille R, Del Pinal F (2005) Wrist MR arthrography: how, why, when. Radiol Clin North Am 43:709–731
48. Yin YM, Evanoff B, Gilula LA, Pilgram TK (1996) Evaluation of selective wrist arthrography of contralateral asymptomatic wrists for symmetric ligamentous defects. Am J Roentgenol 166:1067–1073
49. Theumann N, Favarger N, Schnyder P, Meuli R (2001) Wrist ligament injuries: value of post-arthrography computed tomography. Skeletal Radiol 30:88–93
50. Theumann NH, Pfirrmann CW, Antoni GE, Chung CB, Gilula LA, Trudell DJ, Resnick D (2003) Extrinsic carpal ligaments: normal MR arthrographic appearance in cadavers. Radiology 226:171–179
51. Scheck RJ, Kubitzek C, Hierner R, Szeimies U, Pfluger T, Wilhelm K, Hahn K (1997) The scapholunate interosseous ligament in MR arthrography of the wrist: correlation with non-enhanced MRI and wrist arthroscopy. Skeletal Radiol 26:263–271
52. Schmitt R, Christopoulos G, Meier R, Coblenz G, Frohner S, Lanz U, Krimmer H (2003) Direct MR arthrography of the wrist in comparison with arthroscopy: a prospective study on 125 patients. Fortschr Rontgenstr 175:911–919
53. Saupe N, Prussmann KP, Luechinger R, Bosiger P, Marincek B, Weishaupt D (2005) MR imaging of the wrist: comparison between 1.5- and 3-T MR imaging - preliminary experience. Radiology 234:256–264
54. Kocharian A, Adkins MC, Amrami KK, McGee KP, Rouleau PA, Wenger DE, Ehamn RL, Felmlee JP (2002) Wrist: improved mR imaging with optimized transmit-receive coil design. Radiology 223:870–876
55. Totterman SM, Miller R, Wasserman B, Blebea JS, Rubens DJ (1993) Intrinsic and extrinsic carpal ligaments: evaluation by three-dimensional Fourier transforms MR imaging. AJR Am J Roentgenol 160:117–123
56. Smith DK (1994) Scapholunate interosseous ligament of the wrist: MR appearances in asymptomatic volunteers and arthrographically normal wrists. Radiology 192:217–221
57. Stäbler A, Kohz P, Baumeister RGH, Reiser M (1995) Diagnosis of injuries of the carpal ligaments and capsules using contrast-enhanced MRI. Radiologe 35(Suppl):90
58. Buckwalter JA, Einhorn TA, Bolander ME et al (1996) Healing of musculoskeletal tissues. In: Rockwood CA, Green DP, Bucholz RW et al. (eds) Fractures in adults, 4th edn. Lippincott Raven, Philadelphia, p 261

59. Haims AH, Schweitzer ME, Morrison WB, Deely D, Lange RC, Osterman AL, Bednar JM, Taras JS, Culp RW (2003) Internal derangement of the wrist: indirect MR arthrography versus unenhanced MR imaging. Radiology 227:701–707
60. Herold T, Lenhart M, Held P, Babel M, Ruf S, Feuerbach S, Link J (2001) Indirect MR arthrography of the wrist in the diagnosis of TFCC-lesions. Fortschr Roentgenstr 173:1006–1011
61. Elentuck D, Palmer WE (2004) Direct magnetic resonance arthrography. Eur Radiol 14:1956–1967
62. Kovanlikaya I, Camli D, Cakmakci H, Goktay Y, Kovanlikaya A, Ozaksoy D, Akseki D, Ekin A (1997) Diagnostic value of MR arthrography in detection of intrinsic carpal ligament lesions: use of cine-MR arthrography as a new approach. Eur Radiol 7:1441–1445
63. Stewart NR, Gilula LA (1992) CT of the wrist: a tailored approach. Radiology 183:13–20
64. Boutry N, Lapegue F, Masi L, Claret A, Demondion X, Cotten A (2005) Ultrasonographic evaluation of normal extrinsic and intrinsic carpal ligaments: preliminary experience. Skeletal Radiol 34:513–521
65. Finlay K, Lee R, Friedman L (2004) Ultrasound of intrinsic wrist ligament and triangular fibrocartilage injuries. Skeletal Radiol 33:85–90
66. Griffith JF, Chan DP, Ho PC, Zhao L, Hung LK, Metreweli C (2001) Sonography of the normal scapholunate ligament and scapholunate joint space. J Clin Ultrasound 29:223–229
67. Mohr A, Guermazi A, Genant HK (2003) Value of sonography of the scapholunate ligament. AJR Am J Roentgenol 181:275–277
68. Jacobson JA, Oh E, Propeck T, Jebson PJ, Jamadar DA, Hayes CW (2002) Sonography of the scapholunate ligament in four cadaveric wrists: correlation with MR arthrography and anatomy. AJR Am J Roentgenol 179:523–527
69. Dao KD, Solomon DJ, Shin AY, Puckett ML (2004) The efficacy of ultrasound in the evaluation of dynamic scapholunate ligamentous instability. J Bone Joint Surg 86A:1473–1478
70. Amadio PC (1991) Carpal kinematics and instability: a clinical and anatomic primer. Clin Anat 4:1–12
71. Wright TW, Dobyns JH, Linscheid RL, Macksoud W, Siegert J (1994) Carpal instability non–dissociative. J Hand Surg 19B:763–773
72. Ruby LK, An KN, Linscheid RL, Cooney WP III, Chao EY (1987) The effect of scapholunate ligament section on scapholunate motion. J Hand Surg 12A:767–771
73. Watson K, Weinzweig J, Zeppieri J (1997) The natural progression of scaphoid instability. Hand Clin 13:39–49
74. Watson HK, Ballet FL (1984) The SLAC wrist: scapholunate advanced collapse pattern of degenerative arthritis. J Hand Surg 9A:358–365
75. Palmer AK (1989) Triangular fibrocartilage complex lesions: a classification. J Hand Surg 14A:594–606
76. Taleisnik J (1985) The wrist. Churchill Livingstone, New York
77. Dumontier C, Meyer zu Reckendorf G, Sautel A, Lenoble E, Saffar P, Allieu Y (2001) Radiocarpal dislocations: classification and proposal for treatment: a review of twenty-seven cases. J Bone Joint Surg 83A:212–218
78. Moneim MS, Bolger JT, Omer GE (1985) Radiocarpal dislocation - classification and rationale for management. Clin Orthop 192:199–209
79. Lichtman DM, Bruckner JD, Culp RW, Alexander CE (1993) Palmar midcarpal instability: results of surgical reconstruction. J Hand Surg 18A:307–315
80. Louis DS, Hankin FM, Greene TL (1987) Chronic capitolunate instability. J Bone Joint Surg 69A:950–951